

# Runner profile optimisation of gravitational vortex water turbine

Ridwan Arief Subekti<sup>1,2</sup>, Sastra Kusuma Wijaya<sup>1</sup>, Arief Sudarmaji<sup>1</sup>, Tinton Dwi Atmaja<sup>2</sup>,  
Budi Prawara<sup>3</sup>, Anjar Susatyo<sup>2</sup>, Ahmad Fudholi<sup>2,4</sup>

<sup>1</sup>Department of Physics, Faculty of Mathematics and Natural Sciences, University of Indonesia, Depok, Indonesia

<sup>2</sup>Research Centre for Energy Conversion and Conservation, National Research and Innovation Agency, Jakarta, Indonesia

<sup>3</sup>Research Centre for Electronics and Telecommunication, National Research and Innovation Agency, Bandung, Indonesia

<sup>4</sup>Solar Energy Research Institute, Universiti Kebangsaan Malaysia, Bangi Selangor, Malaysia

## Article Info

### Article history:

Received Oct 31, 2022

Revised Jan 19, 2023

Accepted Feb 3, 2023

### Keywords:

Computational fluid dynamics

Micro hydropower

Numerical optimisation

Potential flow analysis

Propeller-type turbine

Very low head

## ABSTRACT

This study discusses the numerical optimisation and performance testing of the turbine runner profile for the designed gravitational water vortex turbine. The initial design of the turbine runner is optimised using a surface vorticity algorithm coded in MATLAB to obtain the optimal stagger angle. Design validation is carried out using computational fluid dynamics (CFD) Ansys CFX to determine the performance of the turbine runner with the turbulent shear stress transport model. The CFD analysis shows that by optimising the design, the water turbine efficiency increases by about 2.6%. The prototype of the vortex turbine runner is made using a 3D printing machine with resin material. It is later tested in a laboratory-scale experiment that measures the shaft power, shaft torque and turbine efficiency in correspondence with rotational speeds varying from 150 to 650 rpm. Experiment results validate that the optimised runner has an efficiency of 45.3% or about 14% greater than the initial design runner, which has an efficiency of 39.7%.

This is an open access article under the [CC BY-SA](https://creativecommons.org/licenses/by-sa/4.0/) license.



## Corresponding Author:

Sastra Kusuma Wijaya

Department of Physics, Faculty of Mathematics and Natural Sciences, University of Indonesia

Depok, West Java, Indonesia

Email: [skwijaya@sci.ui.ac.id](mailto:skwijaya@sci.ui.ac.id)

## 1. INTRODUCTION

Further research on electrical energy from renewable sources is one increasing energy solution for the increasing demand for global electrification. One of the potential renewable sources in Indonesia is the micro hydro power plant because Indonesia has many rivers. With so many flat contour rivers in Indonesia, micro hydro power plant with a very low head (VLH) is one potential power generation. The gravitational vortex water turbine is one of the renowned water turbines that can be applied to the VLH condition. According to prior research, the average efficiency of the vortex turbine is approximately 14% to 40% [1]–[10]. This efficiency is deemed lower than the conventional propeller turbines, such as the Kaplan turbine that 76% to 84% efficiency [11] or Archimedes screw turbine with roughly 72% efficiency [12].

Several studies have attempted to increase the efficiency of the gravitational vortex turbine, such as by adjusting the number of blades. A vortex turbine with five blades has the highest torque [1]–[8]. Dhakal *et al.* [13] experimentally revealed that the power extracted by the vortex turbine increases as the number of turbine runners is increased to a certain extent. Then, the efficiency decreases when the number of runners is further increased. Khan [14], Dhakal *et al.* [9] and Kueh *et al.* [15] stated that curved runner profiles are more efficient than flat runner profiles. The vortex turbine runner used by Khan [14] is curved in the side view, that by Dhakal *et al.* [9] is curved from the top view, and that used by Kueh *et al.* [15] is

curved at the bottom. Different runner shapes are curved in the crossflow turbine model used by Guzman *et al.* [16]. However, the maximum efficiency obtained is still quite low, around 17.5%.

The addition of baffles to the vortex turbine runner has a significant impact on increasing the efficiency of the vortex turbine, as stated by Sritram and Suntivarakorn [8]. They found that the runner equipped with 50% insulating plates at the top and bottom of the runner has an efficiency reaching 43.83%. Sritram *et al.* [7] studied the effect of turbine materials made of steel and aluminium on the efficiency of a vortex hydroelectric power plant. Their experiments revealed that the maximum efficiency of steel and aluminium turbines is 33.56% and 34.79%, respectively. The torque of the aluminium turbine is higher than that of the steel turbine at approximately 8.4%. Ullah *et al.* [17], [18] investigated the use of runners in more than one stage in vortex turbines. Specifically, they used a three-stage independent (multistage independent) runner with a telescopic shaft. Gautam *et al.* [19] also studied the effect of vortex turbine power by combining several runners on the same shaft. They found that combining the vortex turbine runners into multiplied runners increases the efficiency of the vortex turbine. Experimentally, the power generated by the multiplied runners is 6% greater than the power generated by the single runner. Several studies have also attempted to use conical basins to increase efficiency [3], [17], [18], [20]. Vortex turbines with conical basins create greater power than cylindrical basins. A basin with a logarithmic spiral chamber wall is required for the velocity field to facilitate a transition to an asymmetric distribution of the inlet [21].

The approach on the runner shape optimisation for a vortex turbine is the main problem to be investigated in this study. The numerical optimisation of the performance of the vortex turbine runner profile is conducted using a surface vorticity algorithm to minimise losses to the hydrofoil. Furthermore, the design validation is carried out using computational fluid dynamics (CFD) analysis Ansys CFX to determine water turbine performance. Finally, a vortex turbine prototype with a net head specification of 0.09 m, 400 rpm and water flow rate of 3 l/s has been constructed and tested in the laboratory.

## 2. MATERIALS AND METHODS

### 2.1. Gravitational vortex water turbine architecture

A vortex turbine utilises a whirling fluid (a vortex) as an energy intermediary. For example, river water flow can be directed through the inlet into a carrier channel on the side of the river and find a vortex tank/basin. The vortex tank, which also functions as the turbine housing, has a circular hole at its bottom. The water that comes out from the bottom hole of the vortex tank is redirected into the river through the outlet channel [5], [16], [21]. The working principle of the vortex turbine is as shown in Figure 1. The mathematical concepts related to the flow motion and rotational force in the vortex turbine are governed by the circulation parameter ( $\Gamma$ ) given by (1),

$$\Gamma = 2\pi r v_{\theta} \quad (1)$$

where  $r$  is the distance from the centre of rotation (metre), and  $v_{\theta}$  is the tangential velocity of the fluid at angle  $\theta$  (m/s) [22].

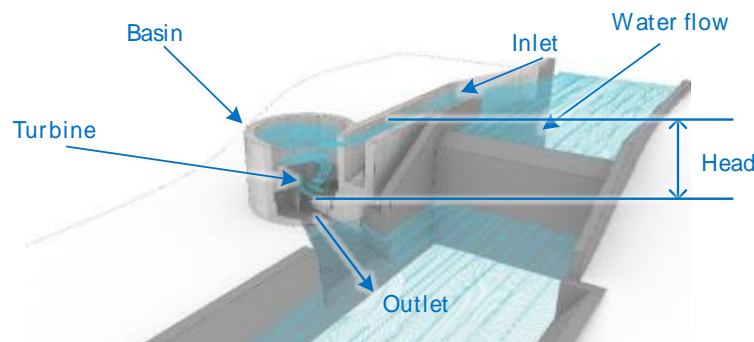


Figure 1. Architecture of gravitational vortex water turbine [23]

The tangential velocity ( $v_{\theta}$ ) in the vortex flow pattern is related to a function of the radius and viscosity [24]. The  $v_{\theta}$  at the inlet of the generator (inlet to the basin) is determined using the continuity (2) and (3).

$$v_{\theta} = \frac{Q}{b h_{in}} \quad (2)$$

$$\Gamma = \frac{2\pi r_{in} Q}{b h_{in}} \quad (3)$$

where  $b$  is the width of the inlet channel, and  $h_{in}$  is the water depth at the inlet channel [25]–[27].

The (3) explains that the vortex strength is highly dependent on the geometric parameter  $r_{in}/b$ , which is denoted as  $\alpha$ . When  $\alpha$  increases,  $r_{in}$  increases or  $b$  decreases. If  $\alpha$  decreases, then  $r_{in}$  decreases or  $b$  increases [25]–[27]. The smaller the inlet width, the higher the efficiency of the vortex turbine [28], [29].

Power *et al.* [5] revealed that the mechanical power output of the water turbine depends on the magnitude of the torque generated by the turbine shaft and depends on the speed of the turbine runner ( $\omega$ ). The input power ( $P_{in}$ ), turbine torque ( $T$ ), output power ( $P_{out}$ ) and turbine efficiency ( $\eta$ ) are calculated using (4) to (8) [5], [30].  $\eta$  increases along with the increase in  $\omega$  and  $T$ , where the amount of  $T$  is affected by the force of the water/force ( $F$ ) hitting the runner at a certain radius ( $r$ ).

$$P_{in} = \rho g H Q \quad (4)$$

$$T = r F \quad (5)$$

$$\omega = \frac{2\pi n}{60} \quad (6)$$

$$P_{out} = \omega T \quad (7)$$

$$\eta = \frac{P_{out}}{P_{in}} 100\% \quad (8)$$

## 2.2. Turbine runner construction

A propeller-type turbine runner is used because it is suitable for VLH applications [31]–[33]. Dietzel [34] explained that the smaller the available head, the fewer the turns of water flow that goes through the runner, and the propeller-type runner has less curvature. In addition, the advantage of the propeller turbine is having a high rotation speed, so that the turbine construction can be made small and can be coupled directly to the generator, thereby reducing mechanical transmission losses [34].

The initial data used in the design of the gravitational vortex turbine components are head (m), water discharge ( $\text{m}^3/\text{s}$ ) and turbine rotation (rpm). The first step in designing turbine components is determining the value of turbine specific speed ( $n_q$ ) by using (9). Specific speed is the number of rotations of the turbine runner working at a water head of 1 m and a water discharge of 1  $\text{m}^3/\text{s}$  [34]. Furthermore, the main dimensions of the gravitational vortex turbine are calculated using (9) to (15) [34].

$$n_q = n \frac{\sqrt{Q}}{H^{0.75}} \quad (9)$$

$$D_1 = \frac{60 v_{\theta}}{\pi n} \quad (10)$$

$$D_N = 0.5 D_1 \quad (11)$$

$$A = (D_1^2 - D_N^2) \frac{\pi}{4} \quad (12)$$

$$D_M = \frac{D_1 + D_N}{2} \quad (13)$$

$$B = \frac{D_1 - D_N}{2} \quad (14)$$

$$L = \frac{D_M \pi}{Z} \quad (15)$$

where  $n_q$  is the specific turbine speed (rpm),  $n$  is the turbine speed (rpm),  $Q$  is the water discharge rate ( $\text{m}^3/\text{s}$ ),  $H$  is the net head (m),  $D_1$  is the runner outside diameter (m),  $v_{\theta}$  is the water tangential velocity,  $D_N$  is the hub diameter (m),  $A$  is the runner cross-sectional area ( $\text{m}^2$ ),  $D_M$  is the diameter of the runner (m),  $B$  is the total runner width (m),  $l$  is the distance among runners (m), and  $Z$  is the number of runner blades.

### 2.3. Surface vorticity modelling

Surface vorticity modelling is an integral method of surface vorticity, which is used to analyse fluid flow. The surface vorticity model can handle potential flows for any situation, including lifting objects, and is the most natural modelling of boundary integral techniques. This modelling offers advantages over the turbine runner profile, which is actually a direct simulation of an ideal fluid flow [35]. The fluid flow that passes through a 2D  $(x, y)$  water turbine runner profile, with uniform flow velocity  $w_\infty$  and slope angle  $\beta_\infty$ , is analysed using the surface vorticity model. The runner exit angle ( $\beta_2$ ), which is the output of the surface vorticity model algorithm, is used to calculate the new stagger angle ( $\xi$ ).

### 2.4. CFD

CFD is used to predict fluid flow, heat transfer, chemical reaction and other phenomena by solving mathematical equations to produce 3D data. The main advantage of CFD is the ability to quickly produce results at a low cost, which makes it suitable for optimisation processes [36], [37]. However, CFD also requires rigorous quantitative validation by physical models before being used because the results from CFD can be higher than the real experimental conditions [37]–[39]. Numerical simulations are carried out using Ansys CFX, which works using the finite volume method on object elements with a 3D water turbine runner model. The used parameters are reference pressure at 1 atm and turbulence model of shear stress transport. The boundary conditions at the inlet use the total pressure, whereas those at the outlet use static pressure. The turbulence numeric is set at a high-resolution type with double precision. Due to the axis-symmetrical runner shape, this study uses turbo mode with one propeller blade model.

### 2.5. Laboratory and experiment set-up

The performance test of the vortex turbine is carried out in the laboratory using a set-up, as illustrated in Figure 2. The circulation pump draws water from the storage tank and flows it into a rectangular intake channel. Water flows through the channel into the basin opening area. The runner is located in the centre of the basin, whereas the outlet hole is located in the centre bottom of the basin. Torque and angular velocity are measured on the turbine shaft. Continuously, water is circulated from the storage tank to the basin and back to the storage tank. The circulation pump is manageable using an inverter to adjust certain water discharges that enter the basin. The head is measured at the end of the rectangular intake channel before entering the basin. Shaft rotation is measured using a digital light-emitting diode (LED) tachometer with a proximity switch as a transducer. Shaft torque is measured using a torque metre to define the output power from the turbine shaft.

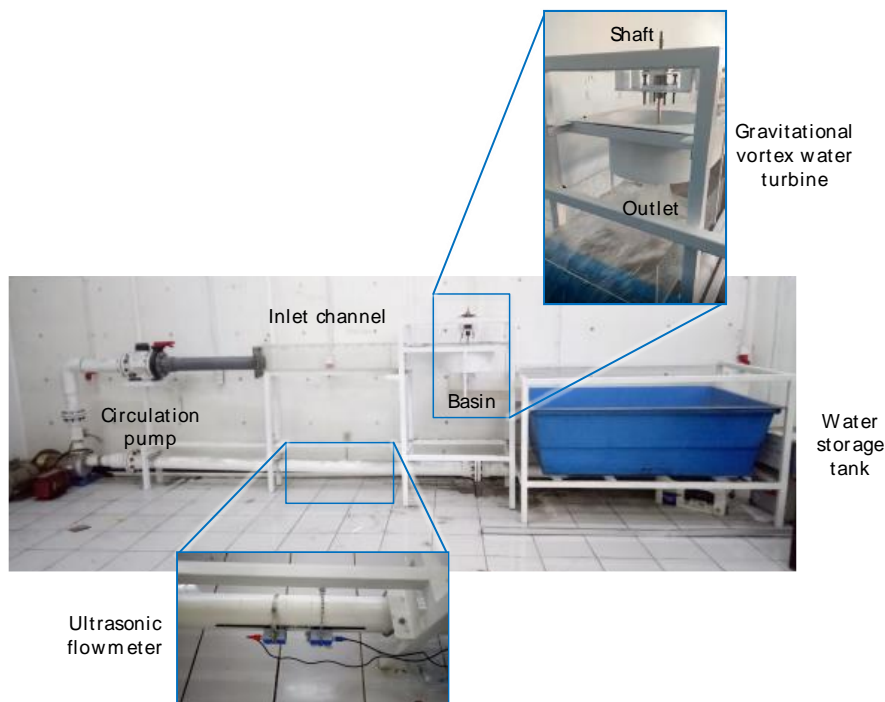


Figure 2. Experimental set-up for the gravitational vortex water turbine

In each test, the water discharge rate is regulated using an inverter and is recorded along with the head, flow rate, torque and no-load shaft rotation. Furthermore, the load on the torque metre is gradually increased. At the stable condition, the torque and shaft rotation are measured. The load on the torque metre continues to be gradually increased until it reaches the maximum torque when the shaft rotation is equal to zero. The specifications for the main measuring tools are shown in Table 1.

Table 1. Instruments for the measurements on turbine performance

Measurement devices	Type	Specification
Ultra sonic flow meter	TUF2000H	Liquid Tester Meter 50 to 700 mm Linearity: 0.5% Accuracy: more than 1% for velocity above 0.2 m/s
Torque Tester	Lutron TQ-8800	Range: 0.01-15.00 kg-cm
Tachometer	Hioki FT 3405	Range of 0.5000 r/s-99990 r/min
Vernier calipers	Mitutoyo, analog, 150 mm	Accuracy 0.05 mm

### 3. RESULTS AND DISCUSSION

This study uses a propeller-type turbine runner because it can mostly operate at the VLH to medium heads [31]–[33]. The turbine is constructed at a laboratory scale with a specification; net head of 0.9 m, velocity at 400 rpm and water discharge rate of 3 l/s. The design of the main turbine dimensions and the basic shape of the runner profile use a speed triangle analysis approach on a 2D profile and is calculated using (9)–(15). The calculation result shows that the maximum power of the turbine is 2.3 W, the specific speed is 133 rpm, the outer diameter of the runner is 94.9 cm, and the diameter of the hub is 47.5 cm. The runner is designed to consist of five blades.

#### 3.1. Turbine runner optimisation

In this study, an analysis of the runner profile is conducted in a 2D water turbine because of the advantages of computing speed compared with a complex 3D analysis. Potential flow analysis using a surface vorticity algorithm coded in MATLAB is carried out, so that losses in the runner profile are minimised. The output of the optimisation algorithm is to determine the optimal amount of runner angle at the water exit ( $\beta_2$ ) to derive the stagger angle ( $\xi$ ). The vortex turbine runner is designed to comprise five profile segments where the profile closest to the hub is segment 1, the middle of the runner is in segment 3, and on the outside of the runner is segment 5. The difference in the stagger angles of the initial and optimised runners using the surface vorticity model algorithm is shown in Table 2.

As presented in Table 2, the initial stagger angle ( $\xi_{initial}$ ) of segment 1 is  $47.48^\circ$ , and the optimised stagger angle ( $\xi_{optimised}$ ) is made to be upright to  $23.71^\circ$ . In segment 2, the difference between the stagger angles ( $\Delta\xi$ ) of the initial and optimised runners is about  $8^\circ$ . In segment 5, the stagger angle of the optimised runner is designed to be slightly larger than that of the initial runner. As a result, both runner designs have a moderately increased stagger angle from segment 1 to segment 5.

Table 2. Stagger angle optimisation on each runner segment

Segment	Stagger on initial runner	Stagger on optimised runner	Stagger difference
	$\xi_{initial}$	$\xi_{optimised}$	$\Delta\xi$
1	47.48	23.71	23.77
2	58.99	50.91	8.08
3	65.48	62.17	3.31
4	69.64	68.33	1.31
5	72.56	73.01	-0.45

#### 3.2. Turbine runner construction

The vortex turbine runner is made using a 3D printer with resin material. The hub section is made separately from the runner to make it easy to install and replace. The propeller-type runner with five blades has an outer diameter of 9.45 cm and a hub diameter of 4.75 cm. The prototype of the vortex turbine runner is shown in Figure 3. The optimised runner design as shown in Figure 3(a) while the optimised runner design which has a more upright profile is shown in Figure 3(b).

#### 3.3. CFD analysis

This section discusses the CFD analysis on the turbine runner only, which is designed to have five blades. The runner blade design is modelled using the Ansys design modeler set in turbo mode because the

runner shape is axis-symmetrical. Turbo mode conducts modelling with one propeller blade model, so that it will speed up the simulation process. The meshing process is initiated using Ansys turbo grid facility with hexahedral structured mesh elements, followed by determining the grid boundary conditions. The details of boundary and continuum conditions to define inlets, outlets, runner blades, hubs and shrouds are presented using CFX-Pre. CFD simulations are conducted on the initial and optimised runners. Both runners are simulated to define the shaft power and then the efficiency. The first CFD simulations are carried out in accordance with various rotational speed variations ranging from 300 to 500 rpm. These limits are in accordance with the specific speed range of the turbine propeller at a predetermined design head and discharge. The second CFD simulations are performed in accordance with variations of water discharges from 2 to 5 l/s.

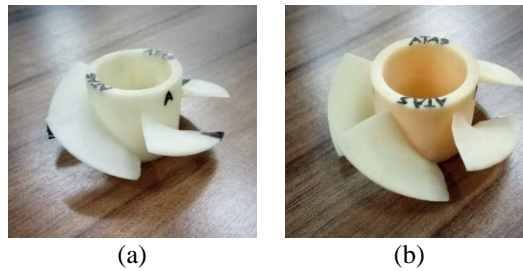


Figure 3. Prototype of the turbine runner (a) initial runner design and (b) optimised runner design

### 3.3.1. CFD analysis on the runner performance to the rotational speed variation

The first CFD analysis is conducted in correspondence with the rotational speed variation (rpm). Figure 4 shows how the shaft power of both runners react to the increase in rotational speed, whereas Figure 5 illustrates the efficiency of both runners in accordance with the increase in rotational speed. The CFD analysis shows that the shaft power of both runners has the same trend; their shaft power increases as the rotational speed increases until it reaches maximum power and decreases even when the rotational speed continues to increase. The optimised runner has a greater shaft power at about 0.72% than the initial runner at a rotational speed of 400 rpm. The efficiency curve line in Figure 5 displays that the efficiency decreases as the rotation speed increases. These results strengthen the previous findings in the research conducted by [12], [15], [40]–[43].

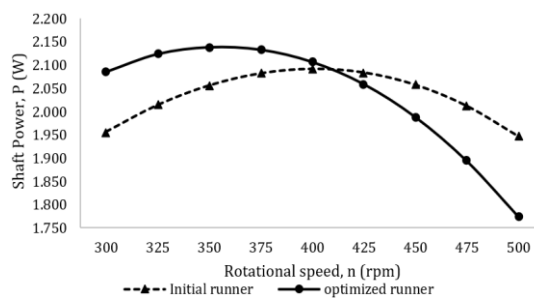


Figure 4. CFD analysis on shaft power to the rotational speed variation of the initial and optimised runners

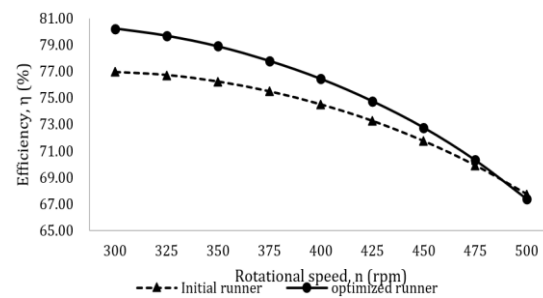


Figure 5. CFD analysis on efficiency to the rotational speed variation of the initial and optimised runners

### 3.3.2. CFD analysis on the runner performance to the water discharge variation

The second CFD analysis is conducted to determine how the optimised runner reacts to the water discharge variation. The simulation is determined to vary the water discharge from 2 to 5 l/s. Figure 6 shows the shaft power analysis on both runners in responding to the increase in water discharge, whereas Figure 7 illustrates the efficiency of both runners when the water discharge increases. Figures 6 and 7 explain that the shaft power and efficiency of both types of turbine designs have the same trend, which has been increasing along with the increase in water discharge. At a discharge rate of 2 l/s, the initial runner has a slightly larger

shaft power than the optimised runner. At a discharge of 2.5 l/s, both runners produce the same shaft power. However, at a discharge rate of 3 to 5 l/s, the optimisation turbine results in a large shaft power as shown in Figure 6. The analysis result is the same as that described by previous researchers [12], [42], [44]–[46].

Figure 7 shows that the optimised runner has a better efficiency than the initial runner, and such efficiency is retained across all water discharge variations. At the point design, namely, at 3 l/s water flow, the optimised runner has 76.4% efficiency, which is 2.6% higher than that of the initial runner. The graph of the water discharge level and efficiency curve of the turbine alone is validated similar to Sritram *et al.* [7] and Rahman *et al.* [28].

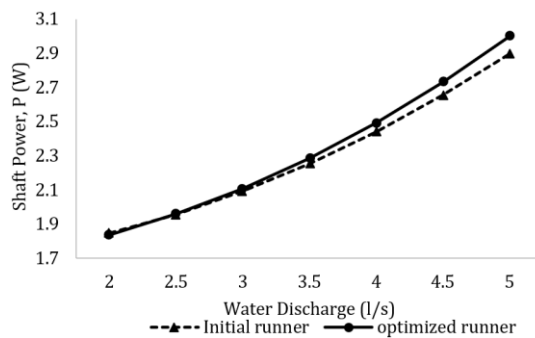


Figure 6. CFD analysis on shaft power to the water discharge variation of the initial and optimised runners

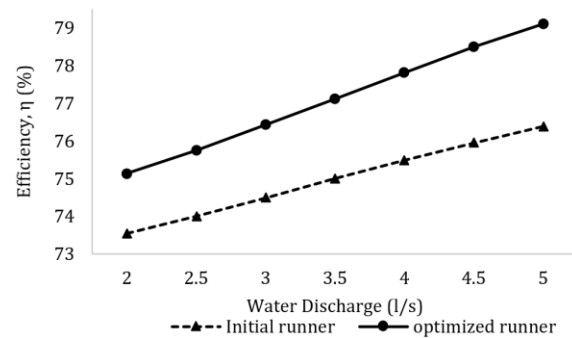


Figure 7. CFD analysis on efficiency to the water discharge variation of the initial and optimised runners

### 3.4. Experimental testing on the vortex water turbine

The experimental testing is performed in a laboratory-scale water turbine prototype, as described in Figure 2. The experiment compares the initial and optimised runners, which are installed in the turbine shaft where the top of the runner is parallel to the floor of the basin. Therefore, upper and lower heads are considered in this experiment. The lower head is measured from the floor of the basin to the centre of the runner, the upper head is the water level in the inlet channel measured to the bottom of the basin, and the total head is the sum of the lower and upper heads.

The optimised runner is physically higher than the initial runner. Therefore, their low heads are different, 1.5 and 1.15 cm, respectively. The initial runner with a water discharge of 3 l/s shows the inlet reading of the water level (upper head) of 17.5 cm, the total head is 18.65 m, and the electric power potential is approximately 5.47 W. Meanwhile, the optimised runner with a water discharge of 3 l/s shows the inlet reading of the water level (upper head) of 17.4 cm, the total head is 18.9 cm, and the electric power potential is 5.55 W. Furthermore, the initial and optimised turbine test results are displayed in the form of a shaft power graph and power torque and finally expressed in an efficiency graph.

#### 3.4.1. Experimental testing on shaft power and shaft torque to the rotational speed

The first experiment is performed to see how the shaft power and shaft torque are affected by a rotational speed variation. The result will later become the basis of the efficiency calculation. Figure 8 shows the measured shaft power and shaft torque on both runners at various rotational speeds from 150 to 650 rpm.

The results show that the vortex turbine with the initial runner has a maximum shaft power of 2,170 W, whereas the turbine with an optimised runner has a maximum shaft power of 2,513 W, which is 15.8% higher than the initial runner. At the maximum turbine rotation, when no load is available, the tachometer reading shows a fairly large value at 661 rpm for the turbine with the initial runner and 646.2 rpm for the turbine with the optimised runner. At the maximum torque, when the turbine rotation is equal to zero, the torque metre reads 14.0 Ncm for the turbine with the initial runner and 14.3 Ncm for the turbine with the optimised runner.

The experiment also confirms that the turbine speed decreases as torque increases. Turbine rotation decreases drastically if the torque is increased high enough. This sudden decrease in turbine rotation is caused by a decrease in the vortex height in the basin, so that the vortex power also decreases. This result is in line with the statement of Khan [14] and Nishi and Inagaki [47] that a decrease in vortex strength causes a decrease in the angular velocity of the blade. One possible conclusion is that a relationship exists between turbine shaft power and turbine shaft torque where an increase in shaft torque incites an increase in shaft



power to the peak point (torque 7.7 Ncm at 269.3 rpm) but will start to decrease if the torque continues increase. This inverted parabolic curve is in accordance with previous studies [4], [9], [14], [19], [45], [47].

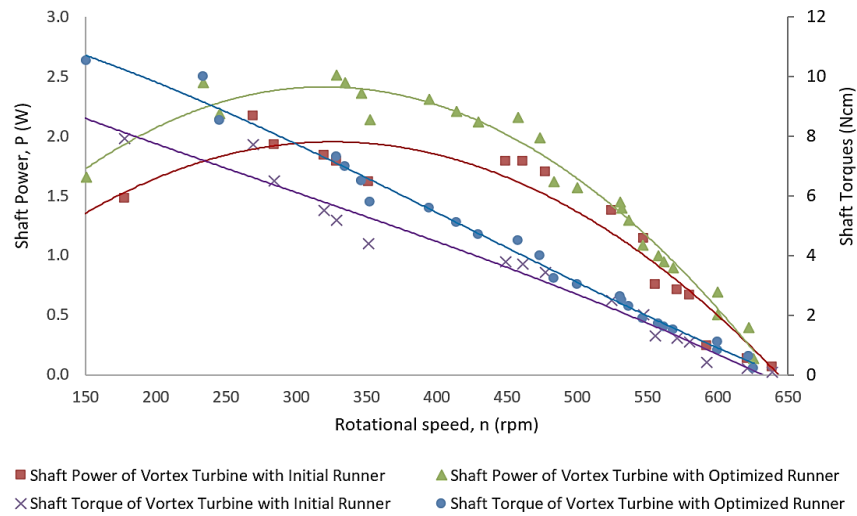


Figure 8. Laboratory experiment results in shaft power and shaft torque to the rotational speed of the vortex turbine with the initial and optimised runners

**3.4.2. Experimental testing on the efficiency to the rotational speed**

The experiments on the efficiency of rotational speed variations have been conducted on both runners, and the result is illustrated in Figure 9. The efficiency of the turbine with the initial runner has the highest efficiency of 39.65% when the torque metre reading is 7.7 Ncm at 269.3 rpm. Meanwhile, the efficiency of the turbine with the optimised runner has the highest efficiency of 45.31%. The efficiency of the optimised turbine is about 14% greater than that of the initial turbine. This result affirms the statement of Saleem *et al.* [6] and Chattha *et al.* [48] that optimising design parameters can produce a strong vortex in the air core, so that the turbine efficiency increases.

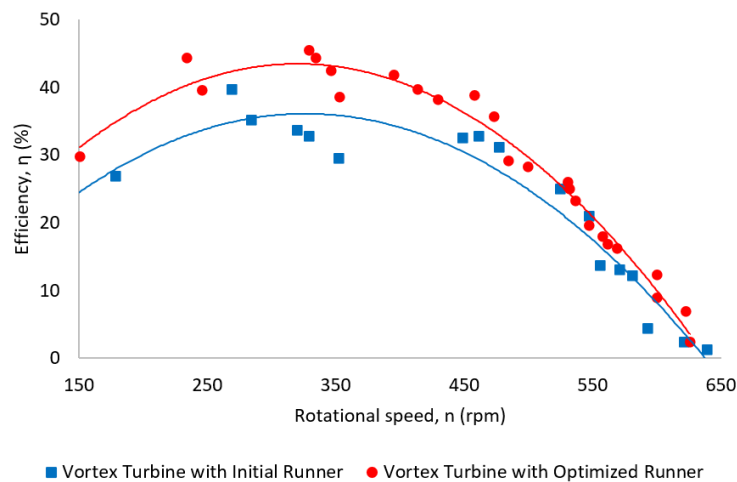


Figure 9. Laboratory experiments result in the efficiency of the rotational speed of the vortex turbine with initial and optimised runners

**3.5. Performance analysis vortex water turbine with an optimised runner**

In this study, the runner used is a propeller-type turbine runner with a certain stagger angle. By adopting a propeller-type runner, the turbine efficiency reaches 45.31%. Tangential and axial forces, which



occur in the vortex turbine basin, can be utilised for energy using a propeller-type runner. Saleem *et al.* [6] revealed that the formed water vortex has two main velocity components, tangential velocity and axial velocity. The tangential velocity component is responsible for the runner vortex movement, and the axial velocity component is responsible for the axial discharge of water from the hole at the bottom of the basin. When the runner is mounted vertically on the hub, only the tangential velocity component of the vortex may be used. However, if the runner is installed at a certain angle, then the water that comes out axially through the hole hits the runner. Thus, the axial velocity component plays its role in rotating the runner. The shaft torque increases when the runner is installed at a certain angle of inclination [6].

The experiment results shown in Figures 4 to 9 confirm that the shaft power and efficiency of both types of turbine designs (with the initial and optimised runners) have the same inverted parabolic curve graph trend. The shaft power and the efficiency have been increased as the rotational speed increased until they reach maximum power and efficiency and then decreased as the rotation continues to increase. Power *et al.* [5] revealed that the mechanical power output of the water turbine depends on the magnitude of the torque generated by the turbine shaft and the angular speed ( $\omega$ ) of the turbine.

#### 4. CONCLUSION

This research has optimised a turbine runner by using the surface vorticity algorithm. The runner is optimised in five segments at a certain stagger angle. The efficiency and power of the optimised turbine are increased compared with those of the initial turbine. The performance of the vortex turbine runner can be viewed by performing CFD analysis on a 3D model with turbo mode. Afterward, the laboratory experiments are carried out on both runner models (initial and optimised designs) to validate the CFD simulations. The simulations reveal that the efficiency of the vortex turbine with an optimised runner is increased at about 2.6% compared with the vortex turbine with an initial runner. Moreover, the turbine optimisation results in great efficiency at all rotational speeds from 300 to 475 rpm. The validation through laboratory testing suggests that the optimised runner has 45.31% efficiency or about 14% greater than the initial runner, which has 39.65% efficiency. The laboratory experiment result strengthens the CFD result that the optimised runner is more efficient than the initial runner. Therefore, the surface vorticity algorithm is successfully deployed as a tool to improve the performance of the vortex turbine runner.

#### ACKNOWLEDGEMENTS

The authors would like to thank the Directorate of Research and Development, Universitas Indonesia under *Hibah* PUTI 2022 (Grant No. NKB-289/UN2.RST/HKP.05.00/2022).

#### REFERENCES




- [1] S. Wanchat, R. Suntivarakorn, S. Wanchat, K. Tonmit, and P. Kayanyiem, "A parametric study of a gravitation vortex power plant," *Advanced Materials Research*, vol. 805–806, pp. 811–817, 2013, doi: 10.4028/www.scientific.net/AMR.805-806.811.
- [2] M. M. Rahman, T. J. Hong, R. Tang, L. L. Sung, and F. B. M. Tamiri, "Experimental study the effects of water pressure and turbine blade lengths & numbers on the model free vortex power generation system," *International Journal of Current Trends in Engineering & Research (IJCTER)*, vol. 2, no. 9, pp. 13–17, 2016.
- [3] S. Dhakal *et al.*, "Comparison of cylindrical and conical basins with optimum position of runner: Gravitational water vortex power plant," *Renewable and Sustainable Energy Reviews*, vol. 48, pp. 662–669, Aug. 2015, doi: 10.1016/j.rser.2015.04.030.
- [4] H. M. Shabara, O. B. Yaakob, Y. M. Ahmed, A. H. Elbatran, and M. S. M. Faddir, "CFD validation for efficient gravitational vortex pool system," *Jurnal Teknologi*, vol. 74, no. 5, May 2015, doi: 10.11113/jt.v74.4648.
- [5] C. Power, A. McNabola, and P. Coughlan, "A parametric experimental investigation of the operating conditions of gravitational vortex hydropower (GVHP)," *Journal of Clean Energy Technologies*, vol. 4, no. 2, pp. 112–119, 2015, doi: 10.7763/JOCET.2016.V4.263.
- [6] A. S. Saleem, Rizwanullah, and T. A. Cheema, "Experimental investigation of various blade configurations of gravitational water vortex turbine (GWVT)," in *2018 International Conference on Power Generation Systems and Renewable Energy Technologies (PGSRET)*, Sep. 2018, pp. 1–5, doi: 10.1109/PGSRET.2018.8685977.
- [7] P. Sritram, W. Treedet, and R. Suntivarakorn, "Effect of turbine materials on power generation efficiency from free water vortex hydro power plant," *IOP Conference Series: Materials Science and Engineering*, vol. 103, Dec. 2015, doi: 10.1088/1757-899X/103/1/012018.
- [8] P. Sritram and R. Suntivarakorn, "The effects of blade number and turbine baffle plates on the efficiency of free-vortex water turbines," *IOP Conference Series: Earth and Environmental Science*, vol. 257, May 2019, doi: 10.1088/1755-1315/257/1/012040.
- [9] R. Dhakal *et al.*, "Computational and experimental investigation of runner for gravitational water vortex power plant," in *2017 IEEE 6th International Conference on Renewable Energy Research and Applications (ICRERA)*, Nov. 2017, pp. 365–373, doi: 10.1109/ICRERA.2017.8191087.
- [10] S. Dhakal, S. Nakarmi, P. Pun, A. B. Thapa, and T. R. Bajracharya, "Development and testing of runner and conical basin for gravitational water vortex power plant," *Journal of the Institute of Engineering*, vol. 10, no. 1, pp. 140–148, Aug. 2014, doi: 10.3126/jie.v10i1.10895.
- [11] S. Waters and G. A. Aggidis, "Over 2000 years in review: revival of the Archimedes screw from pump to turbine," *Renewable and Sustainable Energy Reviews*, vol. 51, pp. 497–505, Nov. 2015, doi: 10.1016/j.rser.2015.06.028.

- [12] J. Rohmer, D. Knittel, G. Sturtzer, D. Flieller, and J. Renaud, "Modeling and experimental results of an archimedes screw turbine," *Renewable Energy*, vol. 94, pp. 136–146, Aug. 2016, doi: 10.1016/j.renene.2016.03.044.
- [13] S. Dhakal, A. B. Timilsina, R. Dhakal, D. Fuyal, T. R. Bajracharya, and H. P. Pandit, "Effect of dominant parameters for conical basin: gravitational water vortex power plant," in *International Conference on Technology and Innovation Management & IOE Graduate Conference*, 2014, pp. 380–386, doi: 10.13140/RG.2.1.1455.7843.
- [14] N. H. Khan, "Blade optimization of gravitational water vortex turbine," Master Thesis, Ghulam Ishaq Khan Institute of Engineering Sciences and Technology, 2016.
- [15] T. C. Kueh, S. L. Beh, Y. S. Ooi, and D. G. Rilling, "Experimental study to the influences of rotational speed and blade shape on water vortex turbine performance," *Journal of Physics: Conference Series*, vol. 822, Apr. 2017, doi: 10.1088/1742-6596/822/1/012066.
- [16] V. J. A. Guzmán, J. A. Glasscock, and F. Whitehouse, "Design and construction of an off-grid gravitational vortex hydropower plant: a case study in rural Peru," *Sustainable Energy Technologies and Assessments*, vol. 35, pp. 131–138, Oct. 2019, doi: 10.1016/j.seta.2019.06.004.
- [17] R. Ullah, T. A. Cheema, A. S. Saleem, S. M. Ahmad, J. A. Chattha, and C. W. Park, "Performance analysis of multi-stage gravitational water vortex turbine," *Energy Conversion and Management*, vol. 198, Oct. 2019, doi: 10.1016/j.enconman.2019.111788.
- [18] R. Ullah, T. A. Cheema, A. S. Saleem, S. M. Ahmad, J. A. Chattha, and C. W. Park, "Preliminary experimental study on multi-stage gravitational water vortex turbine in a conical basin," *Renewable Energy*, vol. 145, pp. 2516–2529, Jan. 2020, doi: 10.1016/j.renene.2019.07.128.
- [19] A. Gautam, A. Sapkota, S. Neupane, J. Dhakal, A. B. Timilsina, and S. R. Shakya, "Study on effect of adding booster runner in conical basin: gravitational water vortex power plant: a numerical and experimental approach," in *IProceedings of OE Graduate Conference 2016*, 2016, vol. 4, pp. 107–113.
- [20] S. R. Sreerag, C. K. Raveendran, and B. S. Jinshah, "Effect of outlet diameter on the performance of gravitational vortex turbine with conical basin," *International Journal of Scientific & Engineering Research*, vol. 7, no. 4, pp. 457–463, 2016.
- [21] A. B. Timilsina, S. Mulligan, and T. R. Bajracharya, "Water vortex hydropower technology: a state-of-the-art review of developmental trends," *Clean Technologies and Environmental Policy*, vol. 20, no. 8, pp. 1737–1760, Oct. 2018, doi: 10.1007/s10098-018-1589-0.
- [22] B. R. Munson, D. F. Young, T. H. Okiishi, and W. W. Huebsch, *Fundamentals of fluid mechanics*. Sixth ed. USA: Don Fowley, 2009.
- [23] Turbulent, "Hydroelectric turbines for green, decentralized, off-grid living," *Turbulent*, 2019. <https://www.turbulent.be/technology> (accessed Jan. 04, 2022).
- [24] M. Azarpira and A. R. Zarrati, "A 3D analytical model for vortex velocity field based on spiral streamline pattern," *Water Science and Engineering*, vol. 12, no. 3, pp. 244–252, Sep. 2019, doi: 10.1016/j.wse.2019.09.001.
- [25] S. Mulligan, J. Casserly, and R. Sherlock, "Effects of geometry on strong free-surface vortices in subcritical approach flows," *Journal of Hydraulic Engineering*, vol. 142, no. 11, Nov. 2016, doi: 10.1061/(ASCE)HY.1943-7900.0001194.
- [26] S. Mulligan, J. Casserly, and R. Sherlock, "Experimental and numerical modelling of free-surface turbulent flows in full air-core water vortices," in *Advances in Hydroinformatics*, 2016, pp. 549–569, doi: 10.1007/978-981-287-615-7\_37.
- [27] S. Mulligan, L. Creedon, J. Casserly, and R. Sherlock, "An improved model for the tangential velocity distribution in strong free-surface vortices: an experimental and theoretical study," *Journal of Hydraulic Research*, vol. 57, no. 4, pp. 547–560, Jul. 2019, doi: 10.1080/00221686.2018.1499050.
- [28] M. M. Rahman, T. J. Hong, and F. M. Tamiri, "Effects of inlet flow rate and penstock's geometry on the performance of gravitational water vortex power plant," in *8th international conference on industrial engineering and operations management, Bandung, Indonesia*, 2018, pp. 2968–2976.
- [29] A. Goude and O. Ågren, "Simulations of a vertical axis turbine in a channel," *Renewable Energy*, vol. 63, pp. 477–485, Mar. 2014, doi: 10.1016/j.renene.2013.09.038.
- [30] A. Harvey, *Micro-hydro design manual*. Rugby, Warwickshire, United Kingdom: Practical Action Publishing, 1993, doi: 10.3362/9781780445472.
- [31] S. J. Williamson, B. H. Stark, and J. D. Booker, "Low head pico hydro turbine selection using a multi-criteria analysis," *Renewable Energy*, vol. 61, pp. 43–50, Jan. 2014, doi: 10.1016/j.renene.2012.06.020.
- [32] A. H. Elbatran, O. B. Yaakob, Y. M. Ahmed, and H. M. Shabara, "Operation, performance and economic analysis of low head micro-hydropower turbines for rural and remote areas: A review," *Renewable and Sustainable Energy Reviews*, vol. 43, pp. 40–50, Mar. 2015, doi: 10.1016/j.rser.2014.11.045.
- [33] M. Technologies, "Kaplan turbine," 2018. <https://www.vlh-turbine.com/products/kaplan-turbine/> (accessed Jan. 06, 2022).
- [34] F. Dietzel, *Turbin, pompa dan kompresor*. Würzburg: Vogel-Verlag, 1980.
- [35] R. I. Lewis, *Vortex element methods for fluid dynamic analysis of engineering systems*. Cambridge University Press, 1991, doi: 10.1017/CBO9780511529542.
- [36] Y. Wang, C. Jiang, and D. Liang, "Investigation of air-core vortex at hydraulic intakes," *Journal of Hydrodynamics*, vol. 22, no. S1, pp. 673–678, Oct. 2010, doi: 10.1016/S1001-6058(10)60017-0.
- [37] T. H. Pulliam and D. W. Zingg, *Fundamental algorithms in computational fluid dynamics*. Cham: Springer International Publishing, 2014, doi: 10.1007/978-3-319-05053-9.
- [38] M. Kayastha, P. Raut, N. K. Subedi, S. T. Ghising, and R. Dhakal, "CFD evaluation of performance of gravitational water vortex turbine at different runner positions," in *KEC Conference*, 2019, pp. 17–25.
- [39] T. C. Kueh, S. L. Beh, D. Rilling, and Y. Ooi, "Numerical analysis of water vortex formation for the water vortex power plant," *International Journal of Innovation, Management and Technology*, vol. 5, no. 2, pp. 111–115, 2014.
- [40] P. Singh and F. Nestmann, "Experimental investigation of the influence of blade height and blade number on the performance of low head axial flow turbines," *Renewable Energy*, vol. 36, no. 1, pp. 272–281, Jan. 2011, doi: 10.1016/j.renene.2010.06.033.
- [41] H. Hoghooghi, M. Durali, and A. Kashef, "A new low-cost swirler for axial micro hydro turbines of low head potential," *Renewable Energy*, vol. 128, pp. 375–390, Dec. 2018, doi: 10.1016/j.renene.2018.05.086.
- [42] H. M. Ramos, M. Simão, and K. N. Kenov, "Low-head energy conversion: A conceptual design and laboratory investigation of a microtubular hydro propeller," *ISRN Mechanical Engineering*, vol. 2012, pp. 1–10, Feb. 2012, doi: 10.5402/2012/846206.
- [43] P. Singh and F. Nestmann, "Experimental optimization of a free vortex propeller runner for micro hydro application," *Experimental Thermal and Fluid Science*, vol. 33, no. 6, pp. 991–1002, Sep. 2009, doi: 10.1016/j.expthermflusci.2009.04.007.
- [44] Y. Bai, F. Kong, S. Yang, K. Chen, and T. Dai, "Effect of blade wrap angle in hydraulic turbine with forward-curved blades," *International Journal of Hydrogen Energy*, vol. 42, no. 29, pp. 18709–18717, Jul. 2017, doi: 10.1016/j.ijhydene.2017.04.185.




- [45] P. Sritram and R. Suintvarakorn, "Comparative study of small hydropower turbine efficiency at low head water," *Energy Procedia*, vol. 138, pp. 646–650, Oct. 2017, doi: 10.1016/j.egypro.2017.10.181.
- [46] J. Titus and B. Ayalur, "Design and fabrication of in-line turbine for pico hydro energy recovery in treated sewage water distribution line," *Energy Procedia*, vol. 156, pp. 133–138, Jan. 2019, doi: 10.1016/j.egypro.2018.11.117.
- [47] Y. Nishi and T. Inagaki, "Performance and flow field of a gravitation vortex type water turbine," *International Journal of Rotating Machinery*, vol. 2017, pp. 1–11, 2017, doi: 10.1155/2017/2610508.
- [48] J. A. Chattha, T. A. Cheema, and N. H. Khan, "Numerical investigation of basin geometries for vortex generation in a gravitational water vortex power plant," in *2017 8th International Renewable Energy Congress (IREC)*, Mar. 2017, pp. 1–5, doi: 10.1109/IREC.2017.7926028.

## BIOGRAPHIES OF AUTHORS






**Ridwan Arief Subekti**    is a researcher in the field of renewable energy at the Research Centre for Electrical Power and Mechatronics, National Research and Innovation Agency (BRIN), Indonesia since 2005 with the current functional position of Researcher Madya. He is currently a member of the Energy Conversion and Conservation Research Group. Completed his undergraduate education in Mechanical Engineering, Trisakti University, Jakarta in 1999, and is currently pursuing his master's degree in the Department of Physics, Faculty of Mathematics and Natural Sciences, University of Indonesia. His research fields are renewable energy, especially water energy, hydro potential survey, preparation of feasibility study (FS), detailed engineering design (DED), techno economic hydro power plant and energy policy. He can be contacted at email: ridwanarief\_rais@yahoo.com.






**Sastra Kusuma Wijaya**    is one of the lecturers in the Department of Physics, University of Indonesia. His expertise is Electronics Instrumentation. He was born in Jakarta on November 26, 1958. He received his Ph.D. from Okayama University, Japan, in the field of the Natural Sciences and Engineering, with a title of dissertation: Mechanical Mobility Technique for Stability and Geometry Assessment of Dental Implant. He has also a strong interest in the Biomedics Instrumentation. Besides actively working as an educator, he also joins to train and manage the Physics Olympiad Team, especially in the experimental discussion, which is one important aspect of the assessment at the International Physics Olympiad. He has also written a number of papers in international journals such as the IEEE Journal. Dr. Sastra Kusuma Wijaya has received several awards such as "The Best Paper Award in the Proc. of the 9<sup>th</sup> Scientific Meeting of the Indonesian Student Association," Tokyo, Japan (2001) as well as "The Outstanding Paper Award in the Proc. ICBME", Singapore (2002). He can be contacted at email: skwijaya@sci.ui.ac.id.






**Arief Sudarmaji**    is senior Lecturer at the Department of Physics, University of Indonesia. Currently serves as Head of the Advanced Physics Laboratory. Some of the publications that have been published include: Calibration of mechanical systems of in-house dynamic thorax phantom for radiotherapy dosimetry, *Journal of Physics: Conference Series* 1528, 012064 (2020), Monitoring distribution system of carbon monoxide and surface ozone based on GPS and microcontroller, *Journal of Physics: Conference Series* 1528, 012023 (2020), and 4f imaging system method to determine optical properties of thin film magnetic material, *AIP Conference Proceedings* 2202, 020029 (2019). He can be contacted at email: arief.sudarmajmy@sci.ui.ac.id.






**Tinton Dwi Atmaja**    started as a researcher at the Indonesian Institute of Sciences (LIPI) in 2005 and is currently a senior researcher at the National Research and Innovation Agency (BRIN). He has been involved in numerous research projects within the scope of renewable energy, energy management system, and microgrid development. He graduated from the Department of Electrical Engineering, Brawijaya University, in 2004 and completed his magister program at Institute Teknologi Bandung in 2010. Meanwhile, he pursued his Doctoral studies at the Centre of Electrical Energy System, Institute of Future Energy, University Teknologi Malaysia. He has published at least eight Scopus-indexed journal articles and more than 17 Scopus-indexed conference papers. He is an Associate Editor in a Scopus-indexed journal, "Journal of Mechatronics, Electrical Power, and Vehicular Technology," and has become a scientific referee in more than 17 reputable journals under Elsevier, Springer, IEEE, Taylor, and Wiley. In addition, he published two books and registered for nearly 12 patents. He has consistently been a member of IEEE PES since 2013 and the member of Indonesian Researcher Union (Himpenindo) since 2013. He can be contacted at email: tinton\_dwi@yahoo.com.






**Budi Prawara**    is senior researcher in Research Organization for Electronics and Informatics, National Research and Innovation Agency (BRIN) since 1997. Doctor of Engineering, University of the Ryukyus, Japan, Material, Energy and Structural Engineering: Post Spray Treatment of Thermal Spray Coating by Spark Plasma Sintering. Research Works in Metal Matrix Composite Coating (2015-now). Influence of SiC Percentage on Microstructure, Microhardness and Oxidation Resistance NiCrBSi-SiC HVOF Coating (Research Collaboration with Surabaya Institute of Technology/ITS), 2018. He can be contacted at email: prawara@yahoo.com.



**Anjar Susatyo**    is a researcher in the field of renewable energy at the Research Centre for Electrical Power and Mechatronics, National Research and Innovation Agency (BRIN), Indonesia since 1996 with the current functional position of Researcher Madya. He is currently a member of the Energy Conversion and Conservation Research Group. Completed his undergraduate education in Mechanical Engineering, Institute of Technology/ITS, Surabaya. He can be contacted at email: anjarsusatyo@gmail.com.



**Ahmad Fudholi**    joined the SERI as a lecturer in 2014. Now, he is Associate Professor in Universiti Kebangsaan Malaysia. He involved ~USD 600,000 worth of research grants (30 grants/project). He supervised and completed more than 40 M.Sc and Ph.D. students. To date, he has managed to supervise eleven Ph.D. (seven as main supervisors and four as co-supervisors). He was also an examiner (three Ph.D. and three M.Sc.). His current research focus is renewable energy, particularly solar energy technology, micropower systems, solar drying systems, and advanced solar thermal systems (solar-assisted drying, solar heat pumps, PVT systems). He has published more than 330 peer-reviewed papers, of which 120 papers are in the WoS index (70 Q1, impact factor of 5-14) and more than 240 papers are in the Scopus index. He has a total citation of 4234 and an h-index of 30 in Scopus. In addition, he has published more than 80 papers at international conferences. He has a total citation more than 6,000, an h-index of 35, and documents of 370 in Google Scholar. He has been appointed as a reviewer of high-impact (Q1) journals, such as Renewable and Sustainable Energy Reviews, Energy Conversion and Management, Applied Energy, Energy and Buildings, Solar Energy, Applied Thermal Engineering, Energy, Industrial Crops and Products, and so on. He has also been appointed as editor of journals. He has received several awards. He owns one patent and two copyrights. He joined the BRIN as a researcher in 2020. He is the best of researcher from ~700 researchers OREM BRIN in 2022. He is World's top 2 % Scientists in 2021 and 2022. He can be contacted at email: a.fudholi@gmail.com.